SEDIMENTOLOGY the journal of the International Association of Sedimentologists

Sedimentology (2023) doi: 10.1111/sed.13154

Soft-sediment deformation structures and Neptunian dykes across a carbonate system: Evidence for an earthquake-related origin (Norian, Dolomia Principale, Southern Alps, Italy)

FABRIZIO BERRA
Dipartimento di Scienze della Terra "A. Desio", Università degli Studi di Milano, Via Mangiagalli 34 20133, Milano, Italy (E-mail: fabrizio.berra@unimi.it)

Associate Editor – Adam McArthur

ABSTRACT

Identification of the processes producing soft-sediment deformation structures, common in siliciclastic deposits and less abundant in carbonate successions, is complex, because different processes may produce similar structures. Thus, interpreting the origin of these structures may be challenging: it requires both a detailed sedimentological study, and the knowledge of the depositional environment and stratigraphic evolution, in order to provide hints to identify the processes affecting sediments after deposition. Among the potential causes of the formation of soft-sediment deformation structures, seismic shock is one of the possibilities, but their origin could be also related to other triggering mechanisms, such as volcanic activity, sediment loading, salt tectonics, fluid expulsion, meteorite impacts and mass movements. Although it is a plausible option, the interpretation of these structures as 'seismites' is not obvious: it must be supported by different lines of evidence, considering that the correct interpretation of soft-sediment deformation structures as a consequence of seismic shocks acquires important implications in palaeoseismology studies. The occurrence of diverse soft-sediment deformation structures in a fault-controlled basin (i.e. in a geological setting characterized by syndepositional tectonics) preserved in different subenvironments of a Norian carbonate system in the Southern Alps of Italy provides the chance to characterize different types of soft-sediment deformation structures along a platform-to-basin depositional profile. Presence of pseudonodules in basinal resedimented limestone, sedimentary dykes and clinostratified breccias with unlithified clasts in slope settings and liquefaction of inner platform facies at the platform top testify to an origin compatible with multiple seismic shocks, repetitively affecting the same stratigraphic intervals. The diverse types of soft-sediment deformation structures in the studied carbonate system provide a rich catalogue of structures related to seismic shocks, representing a possible reference for other similar settings.

Keywords Carbonate platform, seismites, soft-sediment deformation structures, syndepositional tectonics, Triassic.

INTRODUCTION

Soft-sediment deformation structures characterize sediments deposited in various environmental conditions, from continental to deep-water marine settings (e.g. Maltman, 1994). Soft-sediment deformation is recorded by diverse structures, such as slumps, liquified sands, deformed bedding (at diverse scale, from lamination to bedsets), sand injection, sediment-filled fractures (sedimentary dykes), brecciated clast layers, duplex-like structures, sand volcanoes and load casts

(Collinson, 1994). Brittle behaviour documented by breccias and sedimentary dykes may be frequently associated with soft-sediment deformation structures, reflecting the existence of sediments with different degrees of cohesivity and consolidation. Actually, deformation structures change according to the consolidation states of the sediments (Jones, 1994; Cui *et al.*, 2022), but also texture, grain-size distribution and cementation may affect the type and distribution of possible soft-sediment deformation structures (Elliott & Williams, 1988).

Soft-sediment deformation structures form both on the depositional surface and in the shallow subsurface due to various phenomena, mostly related to liquefaction frequently associated with injection of water-saturated sediments and deformation induced by fractures in partly consolidated or cohesive sediments. These structures may have a different origin; therefore, their interpretation in terms of triggering processes (common triggers are earthquakes, volcanic activity, sediment loading, salt tectonics and fluid expulsion; but, also, tsunamis, meteorite impacts and mass movements; Shanmugam, 2016) is challenging. Because similar soft-sediment deformation structures may result from various processes that are able to modify the original texture of sediments after deposition, they cannot be confidently attributed to a specific genetic process. Therefore, the identification of a single soft-sediment deformation structure as a result of a specific kind of all of the possible processes may be speculative (e.g. Cui *et al.*, 2022) without a set of constraints, required to reduce uncertainties on their origin and, eventually, to identify the most plausible triggering process.

In the geological literature, several soft-sediment deformation structures have been uncritically interpreted as generated by earthquakes (Shanmugam, 2016) and named 'seismites', an interpretative term introduced by Seilacher (1969). The impossibility of univocally identifying the triggering mechanism, as well as the morphological convergence of soft-sediment deformation structures produced by different phenomena, led in the geological literature to the abuse of the term 'seismite': the use of a triggering mechanism (earthquake) to describe a deposit is actually misleading (Moretti *et al.*, 2014; Shanmugam, 2016), because earthquakes are only one of the possible mechanisms that could be responsible for the generation of soft-sediment deformations (Owen & Moretti, 2011). Therefore, the correlation between soft-sediment deformation structures and seismic shocks must not be considered obvious.

For these reasons, the interpretation of soft-sediment deformation structures as seismites (*sensu* Seilacher, 1969) is questionable when a detailed sedimentological, palaeogeographical and palaeoenvironmental interpretation of the entire succession where these structures are preserved is missing. Correct interpretation of soft-sediment deformation structures as seismites is critical also because they play an important role for the study of palaeoseismic conditions (Kondo & Owen, 2013).

Development and preservation of soft-sediment structures is strongly related to the nature of sediments. Soft-sediment deformation structures form in almost all of the fine-grained facies types in various depositional environments (Shanmugam, 2017): sandstone, siltstone and claystone (e.g. van Loon, 2009; Owen & Moretti, 2011), evaporites (for example, anhydrite layers; Kirkland & Anderson, 1970; Alsop & Marco, 2011) and carbonates. The highest abundance of these structures is observed in siliciclastic sediments (van Loon, 2009; Owen & Moretti, 2011), where the presence of water and the absence of early cementation create favourable conditions for recording post-depositional deformations, from continental settings to deep water environments. In historical times, earthquake-induced sediment deformations were observed in alluvial plains after major seismic shocks, due to liquefaction of water-saturated deposits, with the creation of fractures and collapses, commonly causing serious damage to infrastructures (for example, 1964 Niigata earthquake; Seed & Idriss, 1967). The effects of seismic shocks in submarine conditions are less evident: nevertheless, the damage of submarine cables associated with major earthquakes (e.g. Heezen & Ewing, 1952) indicates that seismically-induced deformations are recorded at any water depth.

Whereas, in siliciclastic deposits, soft-sediment deformation structures are relatively common (e.g. van Loon, 2009), the situation is different for carbonates: soft-sediment deformations are abundant in slope settings, typically slumps and paraconglomerates (e.g. Moretti *et al.*, 2002; Basilone, 2017), whereas in reefal and inner platform domains their occurrence is rarer (e.g. Pratt, 1994; Spalluto *et al.*, 2007; Ettensohn *et al.*, 2011; El Taki & Pratt, 2012; Chen & Lee, 2013; Morsilli *et al.*, 2020). Experimental tests indicate that carbonates are less affected by soft-sediment deformations than siliciclastic sediments with the same granulometric classes (Pando *et al.*, 2012; Sandoval &

Pando, 2012). Pando *et al.* (2012) verified that calcareous sands are characterized by greater liquefaction resistance than siliciclastic sands, although tested at similar relative densities and consolidation effective stresses. This different behaviour is ascribed to differences in mineralogy, particle shape and porosity (also considering the role of interparticle porosity, typical of carbonate skeletal grains but essentially absent in siliciclastic grains).

With respect to siliciclastic deposits, shallow-water carbonates are typically characterized by early cementation processes. Early cementation is expected to rapidly change the behaviour of carbonate deposits after deposition: complete cementation favours the development of intraformational breccias as well as Neptunian dykes, filled by plastic sediments, indicating partial lithification of sediments during early burial. If cementation is partial, lime-mud-supported rudstone with floating, plastically-deformed soft clasts (Chough & Chen, 2013) may frequently develop.

Detailed investigations of carbonate successions deposited in well-defined geodynamic settings may improve our capability to identify the nature of the triggering processes producing soft-sediment deformation structures in carbonate deposits. This approach has been applied in the Southern Alps to the Norian (Late Triassic) carbonate platform of the Dolomia Principale and coeval basinal succession (Dolomie Zonate and Zorzino Limestone). The abundance of diverse soft-sediment deformation structures and the position at the transition between the inner platform and a fault-controlled intraplatform basin originated by Norian extensional tectonics (Jadoul, 1985; Jadoul *et al.*, 1992; Berra & Jadoul, 1996) provide an ideal setting for the characterization of these structures and the identification of the triggering mechanisms. The existence of a recent 1 : 50 000 geological map (ISPRA, 2012) provides the essential framework to support the sedimentological study.

The aim of the study is to identify, among the various sedimentological structures typical of carbonate platforms and basins, those related to seismic shocks, in order to provide tools for the identification of seismically-induced structures among the soft-sediment deformations and fractures present in carbonate systems.

GEOLOGICAL SETTING

For most of the Norian, sedimentation along the western margin of the Tethys was characterized by a wide, early-dolomitized, attached, inner platform carbonate succession (Dolomia Principale/Hauptdolomit, DP/HD) which is presently preserved in diverse structural/palaeogeographical domains (Marcoux *et al.*, 1993): Southern Alps, Central Austroalpine, Northern Calcareous Alps, Transdanubian Range, Western Carpathians and Central and Southern Apennines. This inner platform was bordered landward by coastal and playa deposits (Keuper in Europe, Grezzoni in the Central Apennine) and towards the Tethys by calcareous backreef and margin facies (Dachstein Limestone) evolving basinward to deep water sediments (Hallstatt Limestone).

During the Middle–Late Norian the Dolomia Principale/Hauptdolomit platform records, in the Central Austroalpine and parts of the Southern Alps, a major tectonic event responsible for the development of rapidly-subsiding, fault-controlled, confined, intraplatform basins (Bechstädt *et al.*, 1978; Jadoul, 1985; Jadoul *et al.*, 1992; Berra, 1995; Berra & Jadoul, 1996; Berra & Jadoul, 1999; Cozzi, 2002; Berra *et al.*, 2010). Syndepositional tectonics is documented by major facies and thickness changes of the Norian succession, that increase from a few hundreds of metres in low-subsiding domains (for example, Dolomites) to more than 2 km in fault-controlled intraplatform troughs. Basinal areas are documented in the Central Southern Alps (Lombardy Basin; Jadoul, 1985; Jadoul *et al.*, 1992; Berra, 1995; Trombetta & Claps, 1995; Berra & Jadoul, 1996; Berra & Jadoul, 1999; Berra *et al.*, 2010; Fig. 1), in the Eastern Southern Alps (Carnia; Cozzi, 2002), in the Central Austroalpine (Ortles and Quattervals Nappes; Berra, 1995; Berra & Jadoul, 1999), in the Northern Calcareous Alps (Seefeld Basin; Fruth & Scherreiks, 1984), in the Apennines (Cirilli *et al.*, 1999; Zamparelli *et al.*, 1999) and in Sicily (Basilone, 2022, and references therein). Sedimentation in the fault-controlled intraplatform basins is mainly characterized by dark, bedded resedimented limestones and scarp breccias (Jadoul, 1985), fed by the Dolomia Principale highs.

In the Western Southern Alps (Lombardy) the Norian basins are asymmetrical (half-grabens; Picotti & Pini, 1988; Jadoul *et al.*, 1992; Trombetta, 1992; Berra & Jadoul, 1996; Fig. 1) and have an average width of less than 20 km (Bertotti, 1991). The fault-controlled transition from the inner platform to the basin is marked by a dolomitized narrow margin dominated by microbialites and serpulids (Berra & Jadoul, 1996; Cirilli *et al.*, 1999), associated with sedimentary dykes. The reef facies rapidly evolve to dolomitized breccia/megabreccia wedges ('Brecce

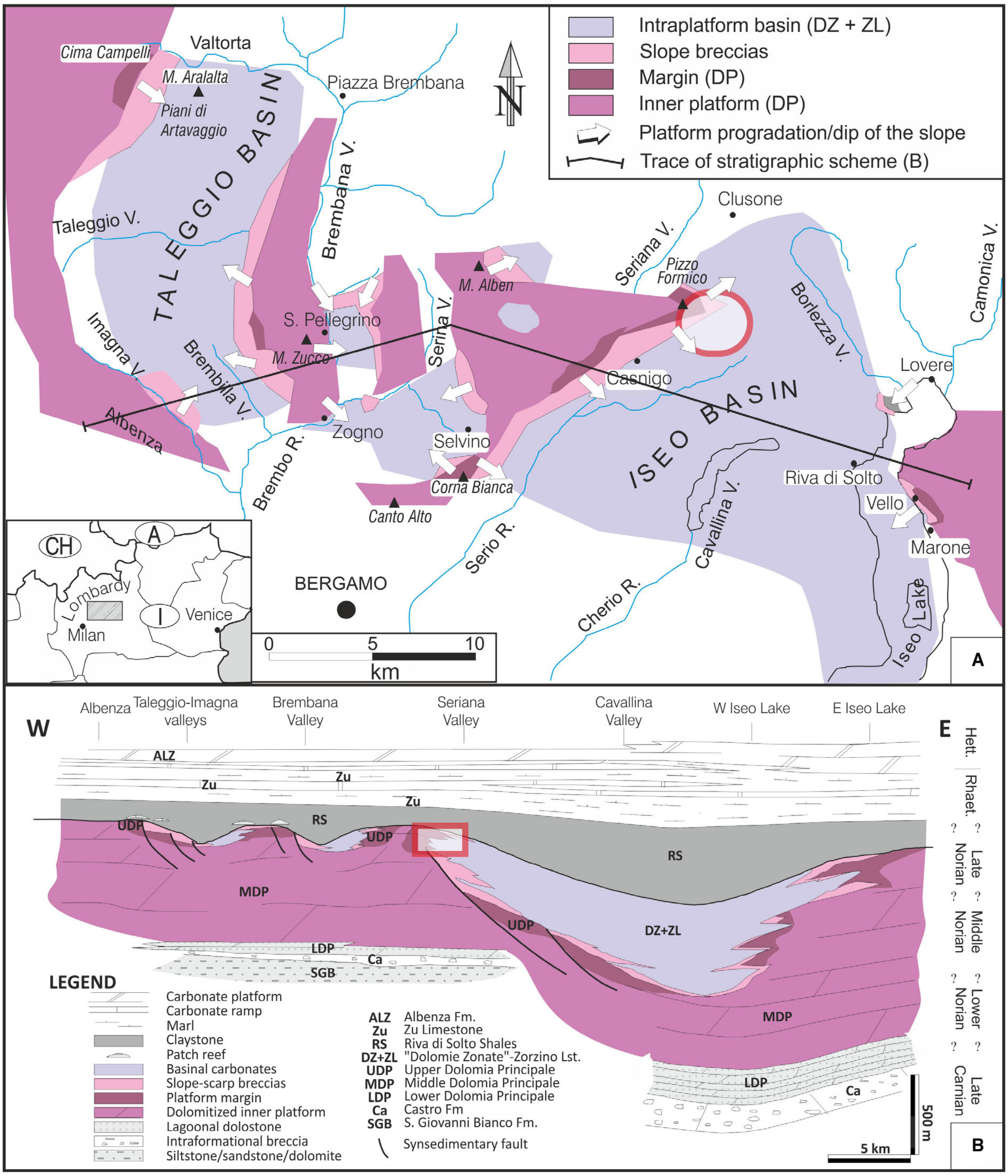

Fig. 1. Palaeogeography of central Lombardy during the deposition of the upper Dolomia Principale with the position of the fault-controlled intraplatform basins (A) and stratigraphic scheme of the area (B). The study area (Pizzo Formico) is marked by the red circle in (A) and box in (B).

sommitali della Dolomia Principale') with angular clasts mainly deriving from the reef and platform top, typically supported by lime-mud.

Basinward, slope breccias interfinger with sand-sized bedded dark dolomitized deposits (packstone and wackestone, Dolomie Zonate) and, more distally, to muddy dark limestones (Zorzino Limestone). In the depocentral area of the larger basins the Zorzino Limestone reaches the thickness of several hundreds of metres, with a maximum of about 1000 m in the Iseo Basin (Assereto & Casati, 1965). The Zorzino Limestone is finest in the depocentral area and becomes gradually coarser towards the borders of the basins, where it interfingers with the Dolomie Zonate and the breccia deposits that characterize the proximal slopes of the Dolomia Principale platform (Bonamini & Berra, 2022). The unit is generally well-bedded, with bed thickness ranging from a few centimetres to, rarely, more than 1 m (Fig. 1). Bioturbation is absent, documenting anoxic bottoms.

The overall evolution of the Norian intraplatform troughs records the tectonically-controlled drowning of parts of the inner platform, with a rapid change from peritidal to subtidal facies. The fault-controlled borders of the basin are the places where the activity of syndepositional tectonics is more evident, in terms of facies and thickness changes, with deposition of breccia layers and wedges associated with slump overfolds in the basinal limestone (Zorzino Limestone) and dolostone (Dolomie Zonate), whose abundance decreases moving away from the basin borders.

The Pizzo Formico area (Figs 2 and 3) preserves the edge of a fault-controlled platform high facing southward an intraplatform basin: slope facies mark the transition between the fault-bounded structural high (horst, footwall) and the platform and slope setting (graben, hangingwall). A typical bioclastic and microbial–serpulid Dolomia Principale margin (Berra & Jadoul, 1996) is preserved, marking the boundary between inner platform facies to the north and slope facies to the south, consisting of clinostratified breccia lenses, fed by the platform high. The transition to distal basinal limestone is cut by a south-dipping Alpine fault, that put in contact bedded dark limestone (Zorzino Limestone) with dolomitized (Dolomie Zonate) proximal slope facies (Fig. 2). The transition between the different facies (inner platform, margin, proximal slope, distal slope) occurs on a distance of less than 1 km: all of these facies record soft-sediment deformation structures and fractures, promoting the observation of coeval, different, post-depositional features in diverse depositional conditions along the depositional profile of a carbonate platform, whose study is expected to provide hints on their nature and to help with identifying the triggering processes responsible for their development.

METHODS

Field work focused on geological mapping (that favoured the identification of major syndepositional and Alpine faults) with sampling of the diverse facies identified in the studied Norian carbonate

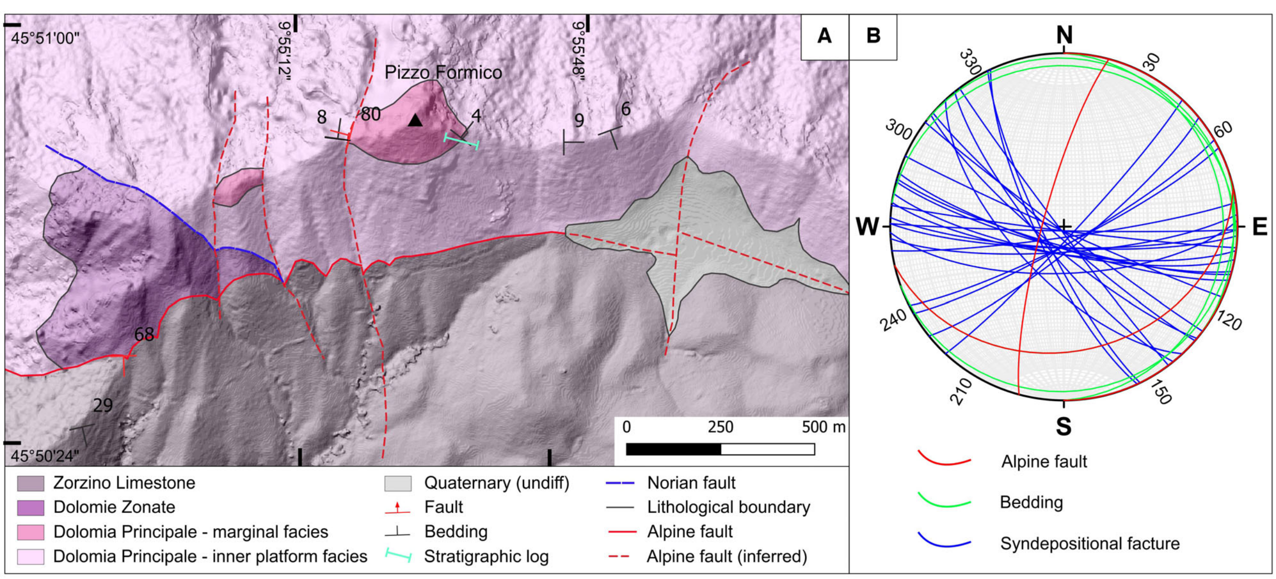

Fig. 2. Geological map of the studied area (A) and stereographic projections (B; equal area, lower hemisphere) of Alpine fault attitude (red), bedding (green) and Neptunian dykes and early fractures (blue).

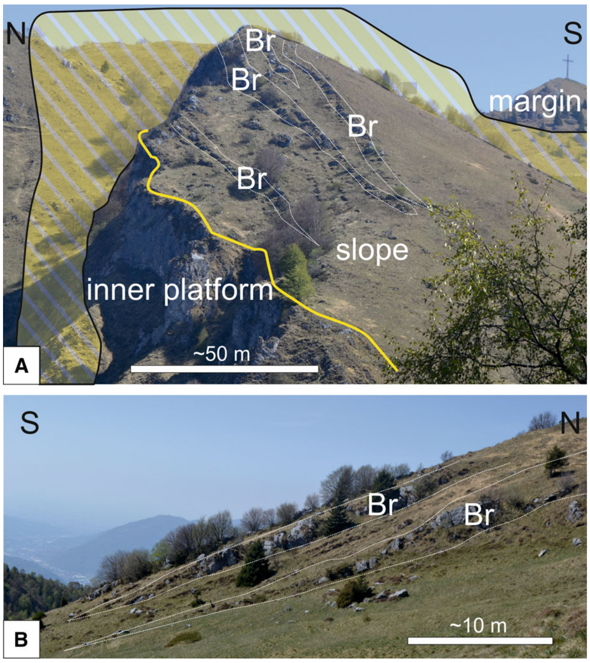

Fig. 3. Geometry of the transition between margin and slope at Pizzo Formico. (A) The increased subsidence in the hangingwall of a Norian normal fault (transparent surface in yellow) led to the deposition of breccias (Br) alternating with bedded dolomitized dark lime-mudstone in the slope facies resting on a thick inner platform succession. Margin facies are preserved in the back (the cross marks the summit of Pizzo Formico). (B) detail of the interfingering of breccia wedges (Br) and bedded dolomitized dark lime-mudstone slope facies on the southern slope of Pizzo Formico, south (hangingwall) of the syndepositional (Norian) normal fault.

systems. Field mapping (Fig. 2) permitted to reconstruct the areal distribution of the facies where soft-sediment deformation structures have been identified. The attitude of early fractures and Neptunian dykes was measured in various outcrops (mostly in inner platform and margin facies), together with the bed attitude and, where possible, attitude of Alpine faults. These data are reported in a stereoplot (Fig. 2). Different types of early/syndepositional deformation structures have been described and then grouped according to the type of deformation and occurrence in different subenvironments of the carbonate systems. Samples were collected for study under a petrographic microscope, focusing on the characterization of facies affected by soft-sediment deformation structures. A stratigraphic log (Fig. 4) crossing the stratigraphic transition between inner platform facies (below) and margin/-upper slope facies (above) at the border of the fault-controlled carbonate high was described (see Fig. 2 for location). Three-dimensional, metre-scale, digital models of selected outcrops from different subenvironments of the carbonate system have been produced (using the software package Polycam®) and are accessible as supplementary material.

TYPES OF SOFT-SEDIMENT DEFORMATION STRUCTURES IN A FAULT-CONTROLLED CARBONATE SYSTEM

Sedimentological analyses focus on post-depositional deformations affecting diverse carbonate sediments with diverse degrees of lithification deposited along a platform-to-basin profile. Soft-sediment deformation structures observed in the studied succession occur in complex associations, but it is possible to identify four endmembers (Fig. 5), according to the physical state of the sediment and the nature of the structures: (i) boudin-like structures; (ii) partly consolidated facies associated with Neptunian dykes; (iii) brittle fractures filled by cements and internal sediments; and (iv) brittle brecciation.

Boudin-like structures

Description. These structures have been observed in the dark, bedded succession of the Zorzino Limestone, consisting of centimetric, well-bedded lime-mudstone with the local presence of decimetric to metric intervals of massive lime-mudstone–wackestone characterized by a pseudonodular texture, with boudin-like structures (Fig. 6). These structures develop in bedsets up to 3 m thick, creating massive intervals within the bedded succession. As a consequence, in the investigated area, the succession

Fig. 4. Stratigraphic log in the upper part of the Dolomia Principale close to the top of Pizzo Formico (see Fig. 2 for position) at the transition between inner platform facies (affected by extensional fault activity documented by Neptunian dykes) and microbial and serpulid marginal facies associated with intraformational breccias, interpreted as evidence of environmental differentiation related to syndepositional tectonics.

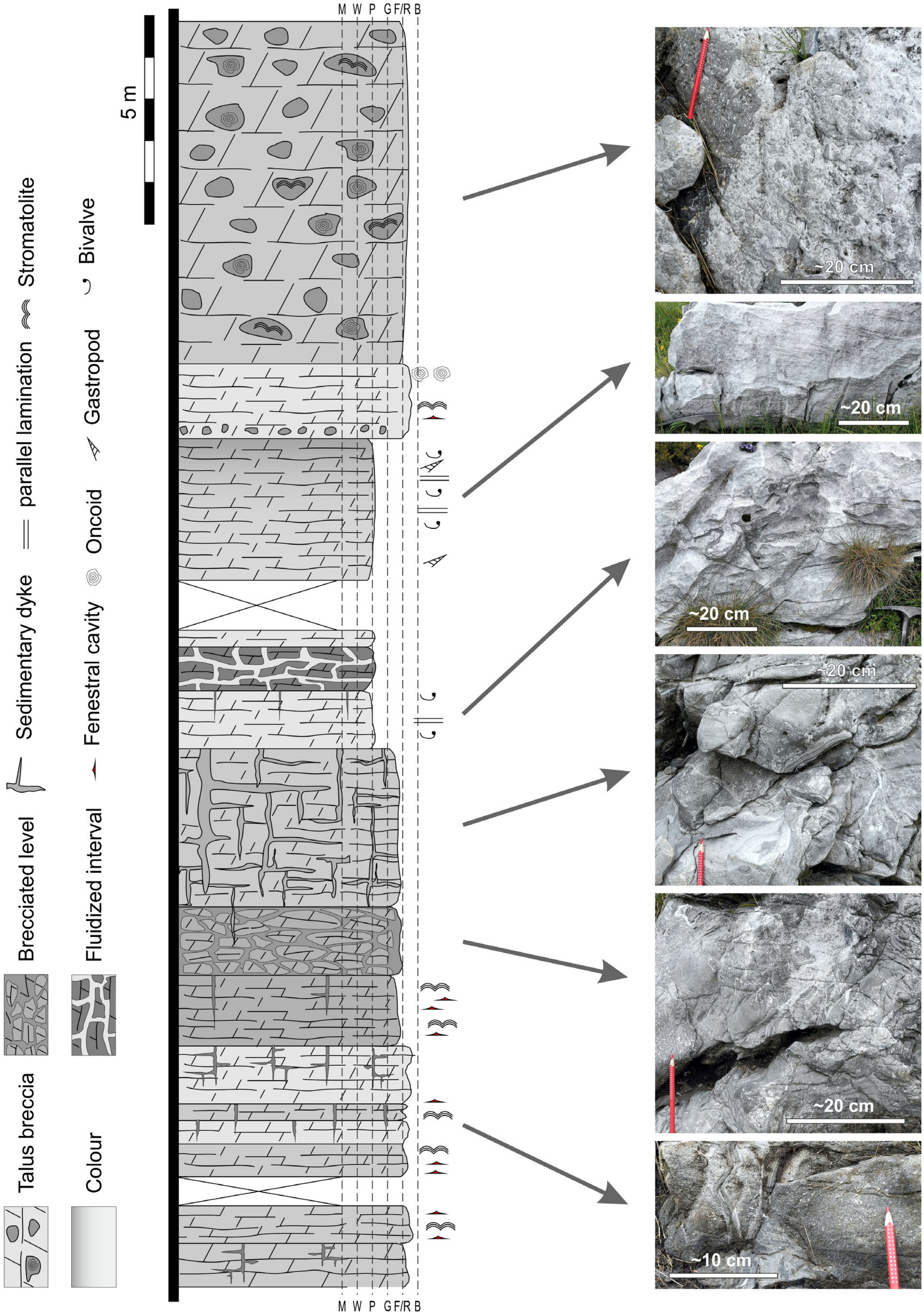

Talus breccia
Brecciated level
Sedimentary dyke
parallel lamination
Stromatolite
Colour
Fluidized interval
Fenestral cavity
Oncoid
Gastropod
Bivalve
5 m
M W P G F/R B
~20 cm
~10 cm

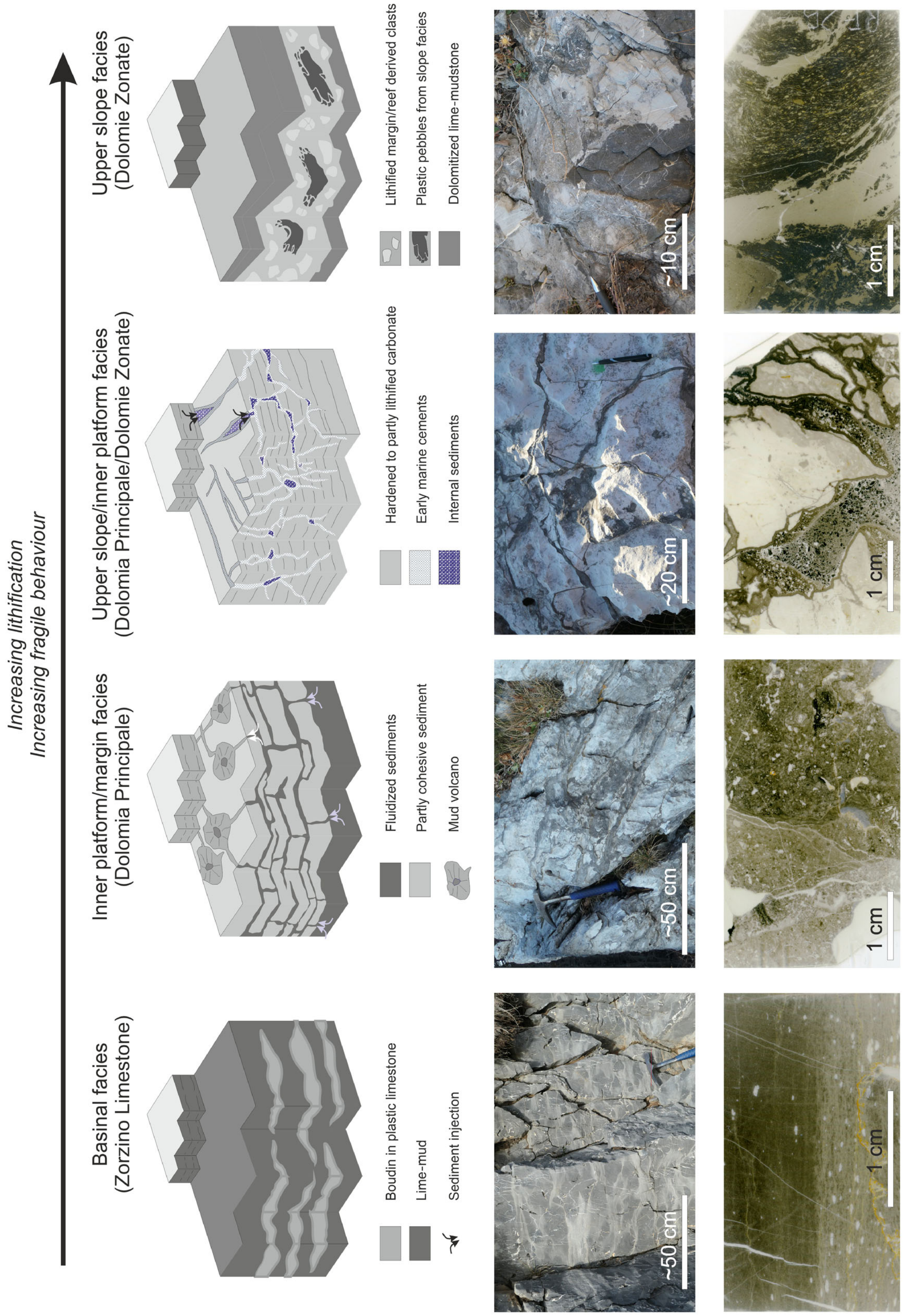

Fig. 5. Main endmembers of the diverse types of soft-sediment deformation structures observed at the fault-controlled transition from inner platform to basinal settings in the Dolomia Principale system at Pizzo Formico. For each type, a schematic sketch, an outcrop image and a thin section is provided.

of the Zorzino Limestone is characterized by prevailing well-bedded, centimetre-thick planar beds alternating with massive intervals consisting of pseudonodular dark limestone.

Interpretation. The features of these deformed intervals are compatible with extensive processes of liquefaction at specific stratigraphic intervals, reflecting the presence of water in the sediment and the transition from a solid to a liquefied state due to the increase of pore-water pressure (Obermeier, 2009), a process generally expected in loosely packed sediments. In these conditions, if the pore pressure is sufficiently high, sediments may be affected not only by liquefaction, but also by fluidization. The distribution of these boudin-like structures is observed only in facies of the Zorzino Limestone closest to the basin margin.

Partly consolidated facies associated with Neptunian dykes

Description. Bedded to massive packstone and wackestone record both plastic deformations and fractures filled by fluidized sediments, interpreted as Neptunian dykes crossing cohesive to plastic carbonate sediments. Neptunian dykes frequently change attitude from vertical, crossing bedded intervals, to horizontal, when they run along bedding surfaces. Neptunian dykes generally dip southwards, with steep inclination (on average about 80°; Fig. 2B). The almost flat attitude of bedding indicates that the present-day attitude of the measured Neptunian dykes roughly represents the original one. Diverse soft-sediment deformation structures are observed in stratigraphic intervals characterized by beds with different competence: Neptunian dykes develop in bioclastic packstone or microbial boundstone, and are filled by lime-mudstone or pellettiferous packstone/wackestone. Locally, forced injection of fluidized sediments in overlying loose to partly loose layers is observed.

Interpretation. The coexistence of plastic deformation and dykes and the different intensity of deformation is likely controlled by the different degree of consolidation, cementation, grain-size and packing of carbonate facies. Injection of liquified sediments in overlying sediments is responsible for the development of 'injectites' (Hurst *et al.*, 2003), which are documented at various burial depths, from very close to the depositional surface up to 500 m (Hurst *et al.*, 2003).

Liquefaction and fluidization may occur for different phenomena: (i) when a load of sediment is rapidly deposited on top of less dense sediments (a situation commonly occurring in case of rapid sedimentation); (ii) because of slope instability not related to seismic shocks; or (iii) in case of ground shaking, typically occurring in case of earthquakes. The first situation can be expected in relatively deep basins, where a massive deposition of sediments may

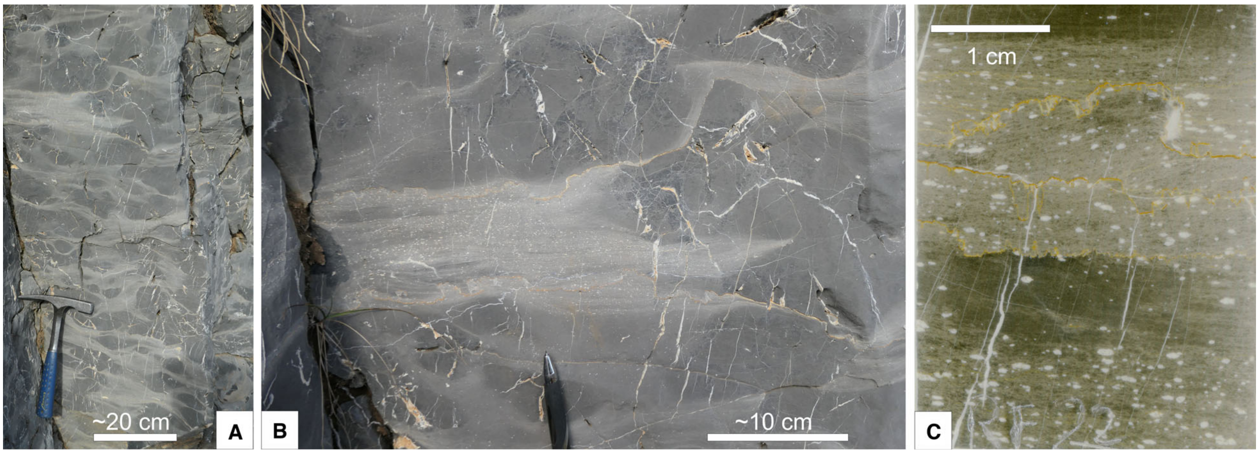

Fig. 6. Soft-sediment deformation structures in basinal deposits (Zorzino Limestone): (A) aspect of a massive layer with a typical pseudonodular/boudinage aspect; (B) detail of the contact between the two different facies (mudstone, dark grey; packstone, light grey) (C) thin section (scan image) with a detail of the transition between the two different facies; the white dots are dolomite crystals recording a partial dolomitization of the basinal limestone. A 3D photogrammetric reconstruction of the outcrop (WGS84 coordinates: 45.8403310 N, 9.9125022 E) can be observed here: https://poly.cam/capture/b37b9ffc-7fd3-4382-9966-a07d96c1a2fe.

load the underlying beds, producing conditions favourable for liquefaction; the second in case of reworking of sediments deposited along an unstable slope; the third is instead possible when saturated sediments are affected by seismic shocks of sufficient magnitude. The complexity of the observed soft-sediment deformation structures associated with fluidization is controlled by the existence of lithologies with different degrees of consolidation (Alsop *et al.*, 2022): the alternation of partly consolidated layers with water saturated loose sediments may explain the observed structures.

Brittle fractures filled by cements and internal sediments

Description. Lithified carbonates (mostly packstone/wackestone and microbial boundstone) are characterized by brittle fractures with sharp borders (commonly associated with angular breccia clasts) filled by fluidized, plastic sediments. This association is interpreted as the typical result of fracturing of completely lithified sediments, with infiltration of lime-mud, producing Neptunian dykes. In the studied succession these dykes range from sub-centimetre to decimetre-scale.

Interpretation. The evolution from loose sediments to lithified deposits occurs by compaction during burial and cementation, the latter being more efficient in carbonate sediments. Lithification may initiate shortly after deposition or later. Lithification is rapid in tropical, shallow-water carbonate deposits and in porous facies, where cementation begins immediately after deposition (e.g. Grammer *et al.*, 1999). It is therefore likely that, due to different permeability and porosity, partly to totally cemented stratigraphic intervals alternated with plastic layers, where cementation has been less efficient. Diverse competence of a sedimentary multilayer is expected to record deformation in diverse ways, independent of their genetic process, generating both brittle and plastic structures. In these conditions, the same stress may cause fractures of hardened sediment and fluidization of loose sediments, that can be injected into fractures. Locally the borders of these fractures are coated by marine cements, documenting a time gap between initial fracturing and sediment injection, occurring only when fractures reach a plastic interval. Size and orientation of the fractures reflect extension normal to the border of the basin (Fig. 2), that can be ascribed to pure gravitational sliding or extensional tectonics.

Brittle brecciation

Description. Strictly, brecciation is not a soft-sediment deformation structure; nevertheless, in the studied succession, it is possible to observe layers consisting of angular clasts embedded in a plastic background, documenting processes able to fracture lithified facies and to mix angular clasts with still plastic sediments, producing matrix-supported breccias. Although brecciation can occur also during burial as a consequence of tectonic stages, in the Pizzo Formico succession, only breccia layers containing both angular and still plastic clasts (which indicate an origin from deformation of consolidated to partly lithified layers), as well as evidence of muddy, fluidized matrix embedding the dispersed clasts, have been considered compatible with soft-sediment deformation structures.

Interpretation. The breccia wedges observed at Pizzo Formico (Fig. 3) can be produced by sliding of lithified clasts from shallower parts of the slope, involving sediments with a diverse degree of cohesiveness and producing a chaotic organization. In other cases, clasts are spaced with complementary margins, documenting *in situ* brecciation, with partial displacement of the clasts, separated by soft-sediments. Neptunian dykes can be present also in the breccia layers, post-dating their deposition.

STRATIGRAPHIC AND PALAEOENVIRONMENTAL DISTRIBUTION OF SOFT-SEDIMENT DEFORMATION STRUCTURES

The Norian succession at Pizzo Formico documents the transition from an inner platform setting to basinal conditions along a fault-controlled slope, recorded by marked facies changes. Both vertical (Fig. 4) and lateral facies changes can be observed, documenting a period of important environmental diversification, related to the Norian extensional tectonics (Jadoul *et al.*, 1992). From basin to top it is possible to identify diverse types of facies associations in the subenvironments of the carbonate system (inner platform to distal basins), each characterized by different depositional and sedimentological characteristics. The qualitative abundance of the observed structures in each subenvironment was evaluated, in order to verify a possible relationship between type of soft-sediment deformation structures and facies.

Basinal facies (Zorzino Limestone)

Description. The basinal facies (Zorzino Limestone) consist of wackestone and packstone passing to prevailing lime-mudstone in the distal parts of the basin. The unit is well-bedded, with tabular beds, frequently laminated. Normally-graded beds are present, more abundant in the proximal part of the basin, close to the toe of the slope (Bonamini & Berra, 2022), documenting resedimentation of inner platform and upper slope sediments. The absence of bioturbation and benthic organisms (as well as the presence of well-preserved vertebrate remains – mostly fish but also reptiles) is indicative of anoxic bottoms. These deposits are frequently affected by post-depositional plastic deformations, mostly represented by slumps (Jadoul, 1985; Bonamini & Berra, 2022). In the Pizzo Formico area, in a position close to the basin borders, some bedsets are instead homogeneously deformed, producing a pseudonodular, boudin-like texture: about 2 m of originally well-bedded limestone shows a pseudonodular aspect, with more cohesive boudins embedded in a plastically deformed matrix (Fig. 6).

Interpretation. Post-depositional deformations in the dark basinal carbonates of the Zorzino Limestone indicate sliding of sediments along a low-angle slope (slumping) as well as liquefaction of sediments with different degree of cohesion on a roughly horizontal sea-bottom. The diverse degree of liquefaction in different beds led to the loss of bed continuity, with a pseudonodular/boudinage texture resulting from the merging of individual beds, likely exposed on the seafloor. Slump overfolds occur both at the lamina and bedding scale, producing typical convolute laminations and bedding, frequently asymmetrical. Their occurrence is not common in the Pizzo Formico area, but frequently observed in the proximal part of the intraplatform basins in nearby outcrops.

Slope facies (Dolomie Zonate)

Description. In the study area, the transition from the platform top to the basin is documented by up to about 3.5 m thick, low-angle clinostratified, massive breccias with abundant lime-mud matrix pinching out in bedded to amalgamated, dolomitized, lime-mudstone to packstone (Fig. 2). Two of the main lithologies, breccias and dolomitized lime-mudstone to packstone, show different texture and record diverse types of depositional processes and post-depositional deformations.

The sedimentological analyses of clinostratified breccias indicate different sources and nature of the intraformational clasts embedded in abundant dolomitized lime-mud. Two types of clasts, ranging in size from a few to about 40 cm, are common: (i) lithified microbial–serpulid boundstone; and (ii) plastically deformed packstone and wackestone (Fig. 7). The aspect of the breccias is chaotic, with clasts embedded in dolomitized lime-mud, where plastic clasts are exploded in small shreds; borders of the unlithified clasts are irregular.

Interpretation. Clinoforms can be interpreted as cohesive, high-density debris flows, deriving from the area proximal to the margin (as documented by microbial–serpulid boundstone in the clasts) and from the slope itself (as documented by the presence of plastically deformed and exploded dark mudstone and wackestone, as well as parts of bedded dolomitized packstone and mudstone). Clasts originated from partly lithified (early-cemented) margin facies and from unconsolidated slope facies involved in the mass flows.

The mixture of lithified and unlithified clasts in the breccias indicates that post-depositional deformation affected facies with diverse degrees of lithification, as documented by the co-occurrence of plastic and brittle deformations found in the clasts. Clinostratified breccias and dolomitized, dark, bedded mudstone are locally affected by a network of fractures filled by different generations of internal sediments (Fig. 8). These fractures document tensional stress affecting lithified to partly lithified sediments: internal sediments, filling these 0.5 to 2.0 cm wide fractures during different episodes, indicate the presence of loose carbonate sediments at the sea-bottom, fluidized and sucked down along these fractures. Clinostratified slope facies thus document two different post-depositional types of deformation: (i) a reworking of a mixture of sediments with diverse degrees of lithification producing massive beds, with a viscous behaviour during deposition, recording mass flows; and (ii) a network of open fractures, filled by soft-sediments, affecting partly lithified lime-mudstone and wackestone, recording extensional stresses affecting early lithified facies at the time of drowning of the inner platform domain.

The deposition of clinostratified subtidal facies covering inner platform and margin facies of the Dolomia Principale at Pizzo Formico

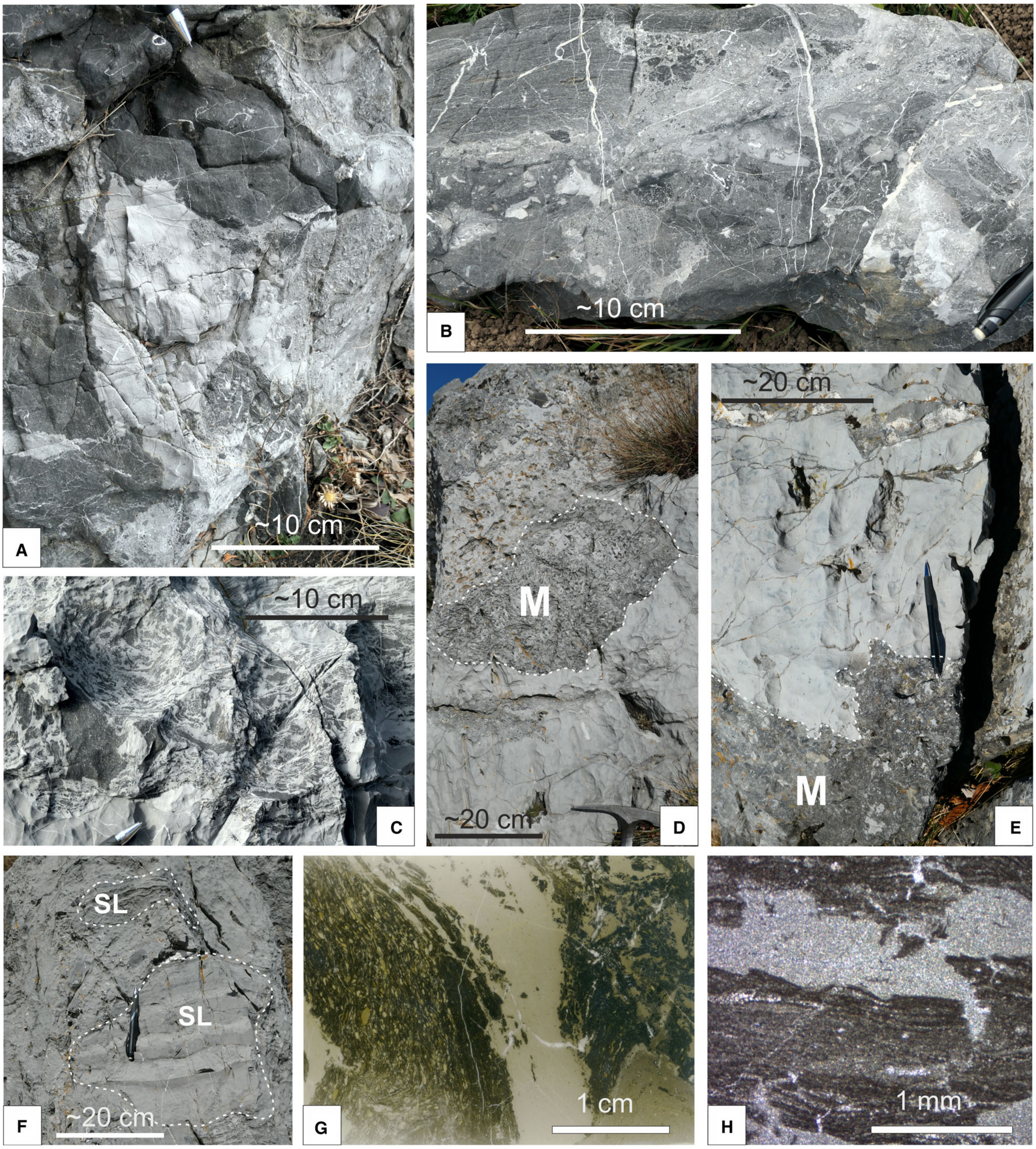

Fig. 7. Aspects of the clinostratified slope breccias (south-western slope of Pizzo Formico, hangingwall of the Norian syndepositional fault). (A) and (B) Examples of dolomitized unsorted breccias with lithified and plastic clasts embedded in abundant lime-mudstone and packstone background; (C) dark plastic clasts exploded in small shreds within a light grey dolomitized lime-mudstone; (D) and (E) margin (microbialite, M) clasts embedded in dolomitized lime-mudstone; (F) two large plastic clasts of bedded slope facies (SL) within a slope breccia; (G) thin section of (C) with a small shred slightly displaced; (H) detail of the texture of the transition between plastic clasts (dark colour) and matrix (lime-mudstone, light grey). All of the facies are mimetically dolomitized. A 3D photogrammetric reconstruction of an outcrop with of dark plastic clasts exploded in small shreds (WGS84 coordinates 45.8432113 N, 9.9142849 E) can be observed here: https://poly.cam/capture/8898c3c6-f30e-4bbd-85d7-5e821dc337ea.

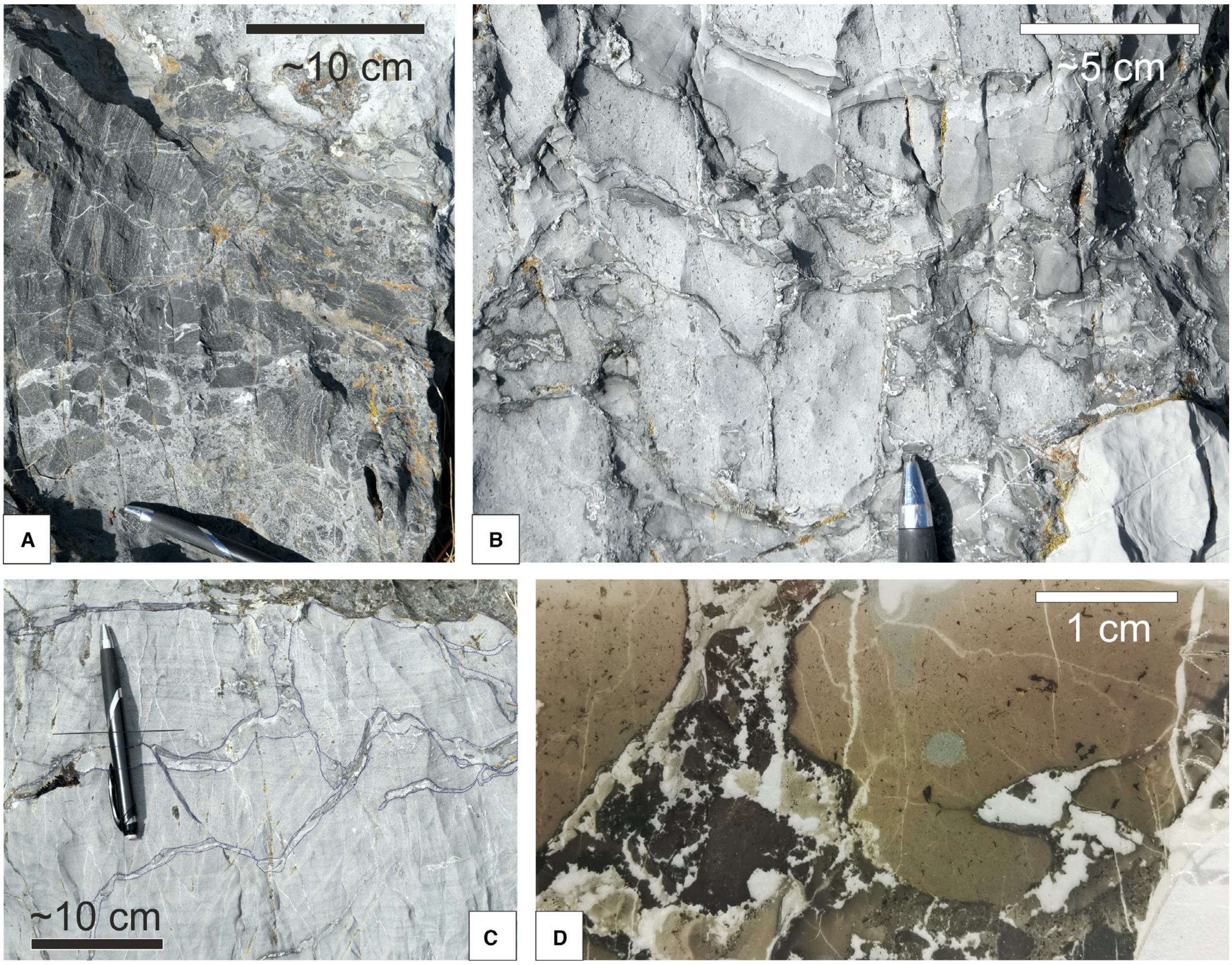

Fig. 8. Texture and structures in the dolomitized slope facies interfingering with the clinostratified slope breccias (south-western slope of Pizzo Formico, hangingwall of the Norian syndepositional fault): (A) dark, plastic deformed bed with initial brecciation; (B) consolidated to partly lithified dolomitized laminated packstone–wackestone affected by a dense network of fractures filled by plastic internal sediments; (C) detail of the laminated dolomitized packstone with sedimentary dykes filled by different generations of internal sediments, documenting a connection of the consolidated slope facies with the sea-bottom where plastic sediments were deposited; (D) thin section of a sedimentary dyke filled by internal sediments with different composition cutting consolidated mudstone. All of the facies are completely dolomitized. A 3D photogrammetric reconstruction of an example of closely-spaced clasts in slope facies (WGS84 coordinates 45.844716 N, 9.915646 E) can be observed here: https://poly.cam/capture/c5f1f82f-9658-4c98-af71-8389989ed803.

(Figs 3 and 4) records a deepening trend, documenting the development of one of the intraplatform basins that characterizes the upper part of the Dolomia Principale (Jadoul *et al.*, 1992). The low angle of clinoforms suggests deposition during the initial stages of basin formation, characterized in the Pizzo Formico area by a limited platform-to-basin relief (likely not more than 100–150 m in the initial stages of basin formation).

Inner platform and marginal area

Description. Soft-sediment deformation structures are present at the platform border facing the intraplatform basin, irregularly affecting stratigraphic intervals in margin and inner platform successions. Carbonate facies, characterized by fabric-retentive early dolomitization that distinguishes all of the Norian inner platform domain of the Western Tethys (Dolomia Principale, Hauptdolomit and equivalent units) are represented by a complex assemblage of bioclastic–intraclastic packstone and wackestone associated with serpulid and microbial (both stromatolitic and oncoidal) boundstone (Berra & Jadoul, 1996; Cirilli *et al.*, 1999; Zamparelli *et al.*, 1999). At Pizzo Formico the transition from inner platform facies to margin facies associated with breccias is observed (Fig. 4), likely recording initial stages of basin formation. These facies record post-depositional deformations, increasing in abundance close to the transition (both vertical and lateral) to slope facies. Deformations can be grouped into two main types: (i) plastically deformed beds with sediment injections; and (ii) sediment-filled dykes (Figs 9 and 10).

Soft sediment deformation structures in these facies document recurring, repetitive events able to generate these deformations in diverse stratigraphic intervals (and, thus, at different times). Plastically deformed beds occur in layers from 2 to 5 m thick, separated by slightly deformed to undeformed intervals, 1 to 3 m thick (Fig. 4): these consist of typical inner platform facies (Fig. 9F), with stromatolitic boundstone associated with subtidal bioclastic–intraclastic packstone and wackestone (Fig. 9D), locally cut by small fractures filled by cements and internal sediments. Alternation of layers with diverse degrees of consolidation and cementation (microbial boundstone and intraclastic packstone and wackestone) reflect a different behaviour, more plastic for packstone and wackestone, more brittle for boundstone. As a consequence, deformed intervals are characterized by a complex, polyphasic network of pockets, dykes and fractures filled by fluidized sediments with diverse characteristics. Fractures and dykes have both sharp and gradual contacts with the host rocks, documenting that they were formed when sediments had diverse degrees of lithification/cementation. In some intervals, plastic behaviour dominates, producing intervals characterized also by injection of sediments, generally consisting of wackestone, lime-mudstone and packstone, from underlying layers in bedded dolostone, producing plastic clasts 'floating' in fluidized sediments (Figs 9 and 10).

In inner platform and margin facies, the presence of brittle fractures and dykes filled by fluidized sediments, frequently with different colour (from light grey to black), is common. Fractures are both vertical and horizontal: horizontal fractures generally follow the bedding surface at the contact between different facies. The final effect is that of a complex set of connected fractures characterized by sharp bending at the transition between vertical and horizontal parts. Dykes and fractures are up to about 5 cm wide: abundance of internal sediments indicates extensional stress, able to create space for the input of plastic sediments from adjoining horizons. Sedimentological evidence indicates that sediments filling the fractures and dykes may derive from unlithified deposits both from above (i.e. younger than the host rock) and from below, from beds less lithified (generally richer in lime-mud) with respect to the overlying fractured interval.

The filling of dykes is frequently polyphasic. In some cases, it is possible to observe a narrow rim of early marine cements (black under cathodoluminescence) pre-dating the input of sediments. The presence of rims of cements along the borders of fractures documents a time gap between fracturing and sediment injection, occurring when fractures reach a plastic interval, after the precipitation of cements on the walls of, at the time, water filled fractures. Sediments filling fractures and dykes are of two types. The most common filling is represented by intraclastic wackestone or lime-mudstone, deriving from mobilization of inner platform sediments from above or below the deformed intervals. The second type of filling consists of dark (frequently black) very fine-grained pellettiferous packstone. This type of internal sediment typically characterizes later fractures and sedimentary dykes with sharp borders, documenting that fractures were formed when the consolidation/lithification degree of the original sediment was sufficient to record brittle behaviour of the host rock.

Interpretation. Plastically deformed beds with sediment injections and sediment-filled dykes may occur together with cross-cutting relationships, recording the effects of different events on the same layers: (i) a first set of events (plastic deformation) occurring immediately after deposition, with sediment still water-saturated and in a plastic state; (ii) a second set of events affecting carbonate deposits after the achievement of a competence sufficient to produce a brittle behaviour. Occurrence of multiple events affecting layers at different times, with diverse degrees of lithification/cementation, indicates the existence of repetitive processes, acting in the same stratigraphic interval, recording the gradual consolidation/cementation of sediments and producing different structures due to the increasing degree of lithification with time. Pellettiferous packstone filling later fractures is not present in the inner platform succession, suggesting that these sediments were likely endogenous: no detailed data are available,

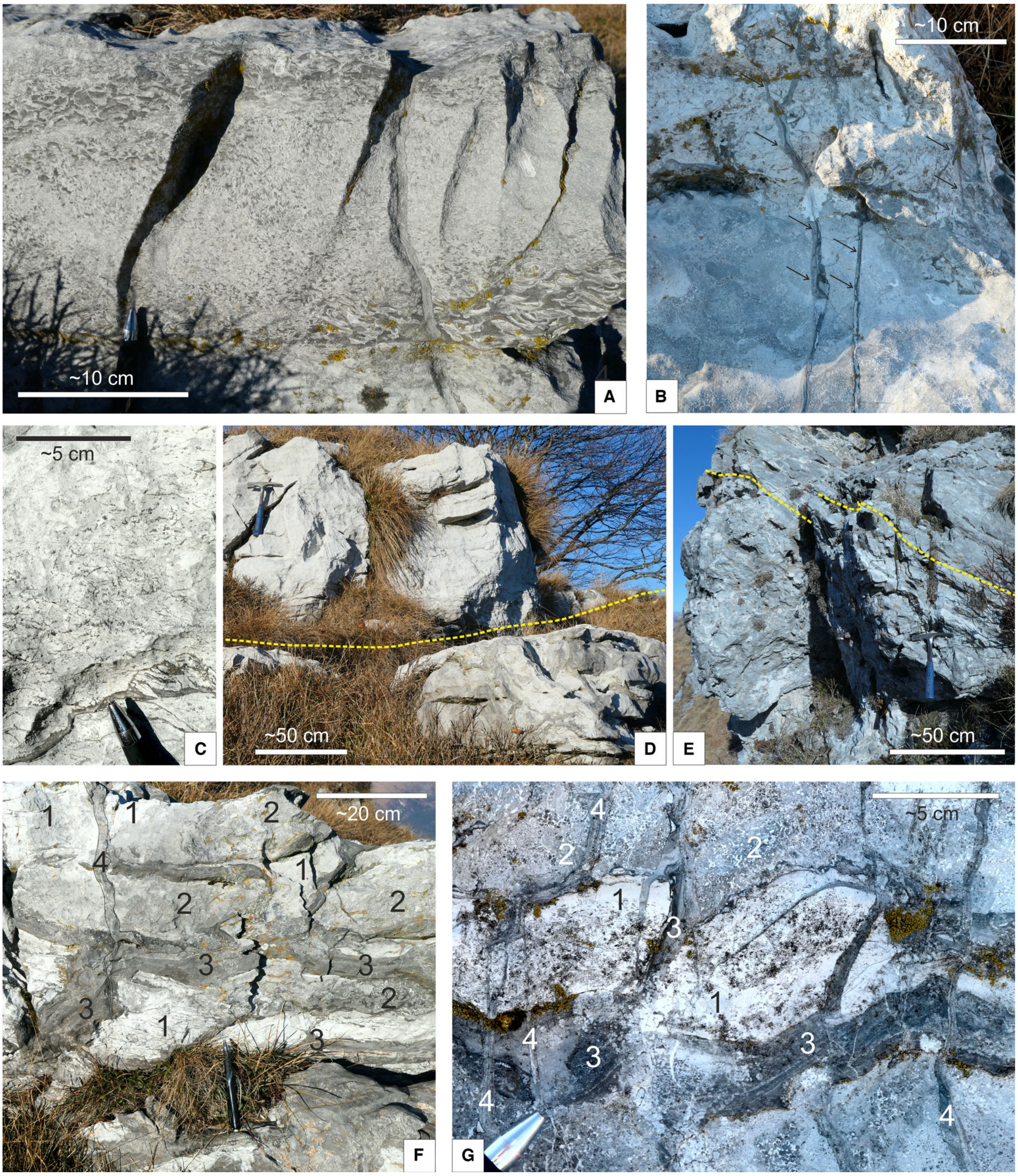

Fig. 9. Facies associations and soft-sediment deformation structures on the platform top (inner platform and margin facies; summit of Pizzo Formico and eastern ridge): (A) graded bioclastic (mostly floated bivalves) dolostone, interpreted as probable tempestite; (B) contact between a bioclastic rudstone (light colour, above) and a microbial boundstone, both crossed by small extensional fractures (arrows) filled with dark mudstone–pellettiferous packstone; (C) microbial fenestral boundstone, intertidal deposits; (D) contact between undeformed intra-bioclastic packstone above a stratigraphic interval affected by different generations of fractures filled by internal sediments; (E) contact between microbial boundstone (above) and a chaotic, plastically deformed subtidal interval; (F) multistage soft-sediment deformations in light coloured poorly bedded packstone (1) and microbial boundstone (2) cut by fractures filled by dark liquified sediments (3) later crossed by later fractures (4); (G) plastic to brittle deformations in inner platform sediments, with light-coloured packstone (1) and microbial boundstone (2) cut by fractures filled by dark, liquified sediments injected from below (3), later crossed by fractures filled by cements and internal sediments (4).

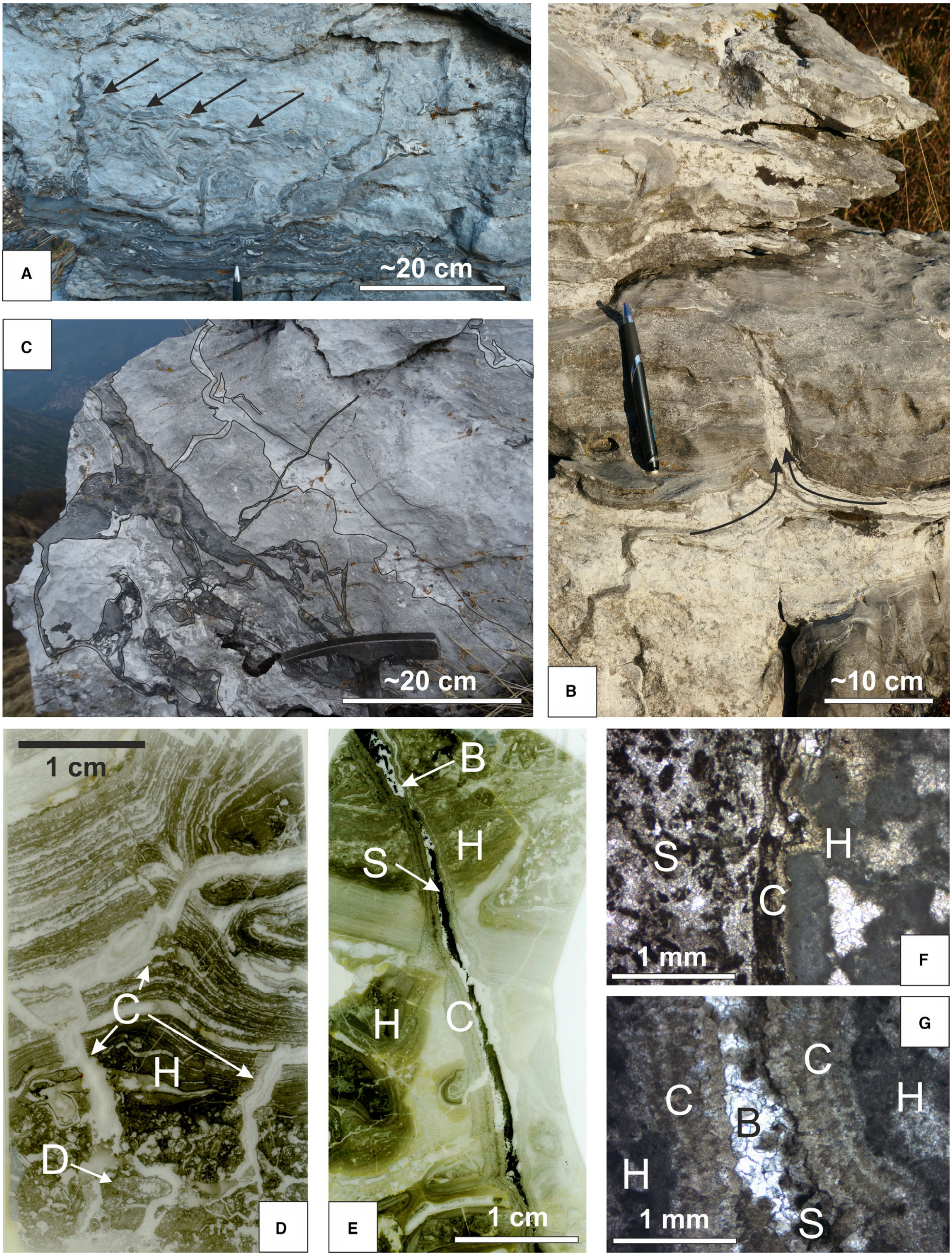
A
~20 cm
C
~20 cm
B
~10 cm
1 cm
C
H
D
B
S
H
H
C
1 cm
E
S
H
C
1 mm
F
G
C
C
B
H
H
S
1 mm

Fig. 10. Examples of multiple cross-cutting relationships among different generations of soft-sediment deformation structures at Pizzo Formico; inner platform and margin facies, eastern and western ridge of Pizzo Formico: (A) fluidization of laminated sediments (arrows) later crossed by plastic to brittle fractures injected by dark sediments from the underlying layer; (B) inner platform sediments with fractures filled by fluidized sediments injected from a more plastic layer below (arrows); (C) multiple fractures crossing, at different times, the same stratigraphic interval, with injection of liquified sediments with different colouration; (D) thin sections of microbial boundstone ('H') covering intra-bioclastic packstone (with a dasycladacean algae crossed by small open fractures filled by early marine cements, (E) thin section of a (D) detail of a fracture crossing a cemented dolomitized microbial boundstone ('H'): the fracture is characterized by fibrous cements at the borders and black internal sediments, locally with dolomitized blocky cements; (F) and (G) detail of fractures crossing microbial boundstone ('H') in inner platform facies: the borders of the fractures are coated with cements ('C') more developed in (G) and filled by internal peloidal sediments ('S') and dolomitized blocky cements ('B'). A 3D photogrammetric reconstruction of soft-sediment deformation structures on the platform top (WGS84 coordinates 45.8465792 N, 9.9197040 E) can be observed here: https://poly.cam/capture/a068e97c-81e6-4fe3-8188-4f4ecc658a32.

but its origin could be related to the existence of cavities, where these sediments (likely related to organic activity) were formed, before arriving in the fractures, initially only filled by water, as documented by rims of early marine cements.

DISCUSSION

Trigger mechanism recognition

From structures to processes

Interpreting the origin of soft-sediment deformation structures is challenging because various processes can produce similar structures and textures: this is especially complex when soft-sediment deformation structures are isolated – either of a single type or limited to a single depositional setting – because diverse processes may be responsible for their development. The co-occurrence of diverse soft-sediment deformation structures in the same stratigraphic interval and depositional system may instead help in reducing the uncertainties about their origin. Evidence of soft-sediment deformation structures interpreted explicitly as seismites in carbonate successions are relatively common, although their occurrence is frequently documented episodically in specific positions within the depositional system, such as in cores (Hou *et al.*, 2020; Zhang *et al.*, 2022), preventing the reconstruction of the lateral distribution of these structures across different subenvironments of carbonate platforms. Most of the structures are represented by brecciation and deformed laminations. Evidence of deformation interpreted as seismites is also reported from outcrops (e.g. Wallace & Eyles, 2015; who interpreted deformed rhythmically laminated dolostones as related to slumping of lagoonal facies from bioherms). The existence of conditions that favour the preservation of a diversified set of soft-sediment deformation structures on a reasonably short distance (1 to 3 km) is not common, so the present case study could represent an interesting example of how detailed sedimentological investigations may help in identifying the origin of diverse soft-sediment deformation structures preserved along the depositional profile of a carbonate platform.

The studied succession, recording the transition from platform top to basin across a fault-controlled margin (Fig. 11), provides exceptional conditions for studying diverse types of deformations and their associations, producing constraints for the identification of the events producing the observed soft-sediment deformation structures. In detail, favourable conditions occur when: (i) environmental constraints allow the exclusion of some of the possible causes of soft-sediment deformation structures, reducing the uncertainties on their origin; (ii) diverse types of soft-sediment deformation structures are observed in different subenvironments of a depositional system, such as in the study case; (iii) different types of post-depositional deformation are observed in different facies types, therefore it is expected that the same type of deformation process may produce different post-depositional deformations documented by diverse sedimentological structures.

Origin of soft-sediment deformation structures at Pizzo Formico

Occurrence of pseudonodular intervals with boudin-like deformations in resedimented facies of the Zorzino Limestone is considered as the effect of partial liquefaction of cohesive resedimented limestone resting on a roughly flat depositional surface due to shaking, which can be ascribed to diverse processes: likely seismic shocks, but also meteorite impacts, gravity-driven mass movement and tsunamis or internal waves. Soft-sediment deformation structures are also observed in slope facies, where evidence of resedimentation from the upper part of the slope is documented by clasts containing serpulid and microbial boundstone. This instability involves both hardened facies (typically microbial boundstone) and unlithified but cohesive facies, whose reworking generates soft clasts embedded in abundant dolomitized lime-mudstone. This facies reflects mass movement (slope failures) along the slope connecting platform top and basin. Instability can be ascribed to physiological collapses along high-sedimentation slopes but also to major storms, internal waves or seismic shocks. The involvement of upper slope boundstone (already cemented or lithified) suggests that mass flow also affects the lithified slope facies, and not only the muddiest parts, pointing to tectonics (Jadoul, 1985; Jadoul *et al.*, 1992) as the most plausible cause, typically associated with seismic shocks. The presence of open fractures filled by internal sediments (post-dating a partial

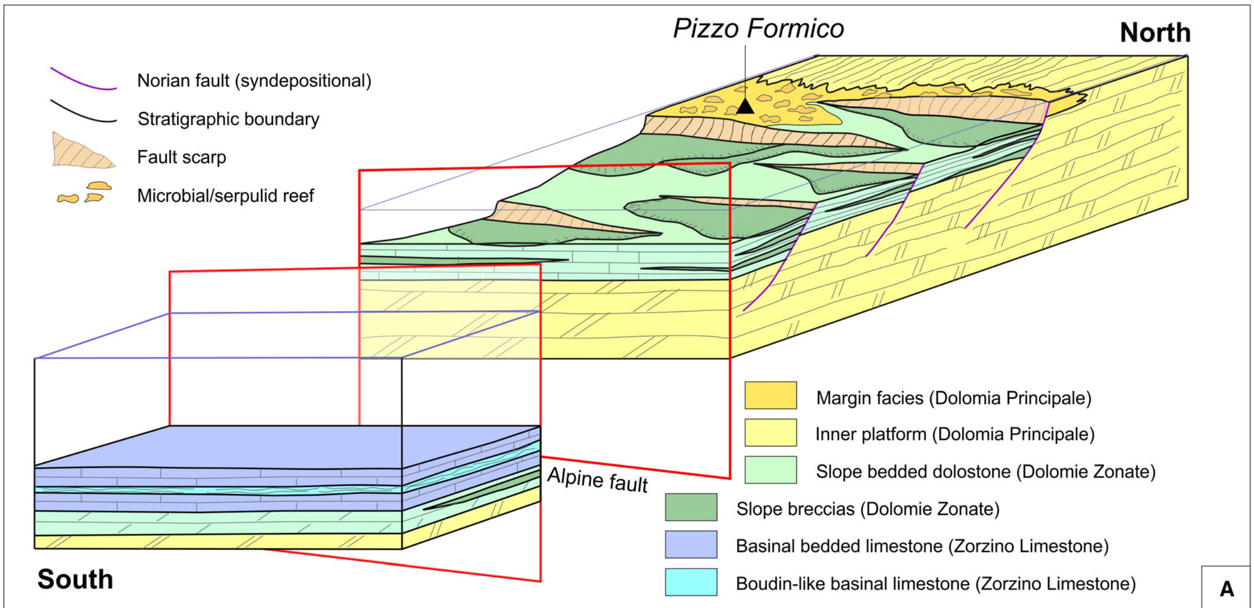

B

		Types of soft-sediment deformation structures										
PREVAILING FACIES	**DEPOSITIONAL ENVIRONMENT**	slump fold	sediment injection	pseudonodule	convolute laminations	convolute bedding	microfolds	extensional fault	neptunian dyke	bouden	brecciated clast	tensional fracture
microbial boundstone (dolomitized)	inner platform/ margin		C		P		C	C	C	C	C	C
dolomitzed, light-grey packstone/wackestone	inner platform (subtidal)		C	R	P		C	P	C	R	P	P
mud-supported breccias (dolomitized)	slope facies (clinoforms)		P					C	C	C	C	C
dark grey dolomitized lime-mudstone	slope facies (bedded dolostone)	R	R					R				
bedded to massive packstone/ wackestone (dolomitized)	proximal basin	P	R	P			R			R	R	
black, thin-bedded packstone to lime-mudstone	distal basin	C	R	P	C	C	C			R		

Common: C
Present: P
Rare: R

Fig. 11. (A) Palaeogeographical reconstruction of the study area, with the representation of the different subenvironments along the platform-to-basin profile at Pizzo Formico. (B) Type, distribution and abundance of soft-sediment deformation structures in the different facies and subenvironments identified in the Norian carbonate system at Pizzo Formico (from the inner platform facies of the Dolomia Principale to the intraplatform basins where the basinal carbonates of the Zorzino Limestone were deposited) are summarized.

lithification of the reworked slope facies) reflects an extensional tectonic setting, further supporting a control by the well-known syndepositional extensional tectonics, eventually leading to the development of inner platform basins in the Dolomia Principale depositional system (Jadoul *et al.*, 1992). Although slumps may originate by sliding of unconsolidated sediments and breccias by submarine rockfalls, both possibly without fault impetus, the documented syndepositional tectonic activity suggests that at least some of the observed structures may have been triggered by seismically-induced instability. Of course, it is impossible to refer each slump and similar soft-sediment deformation structure to one of the possible processes able to trigger sliding along the slope. An origin related to seismic shocks is likely for fluidized and liquified sediments, such as the boudin-like structures in the Zorzino Limestone, the partly consolidated facies associated with Neptunian dykes and the plastic filling of Neptunian dykes (e.g. Bourrouilh *et al.*, 1998; Wendt, 2017).

Whereas mass movement can explain several types of soft-sediment deformation, structures in slope and basinal facies (where gravity alone may trigger reworking of previously deposited sediments), similar mass movements are not possible on the platform top, where the depositional surface is horizontal. The presence of stratigraphic intervals affected by liquefaction and fractures filled by sediments (Neptunian dykes) alternating with intervals consisting of almost undeformed subtidal–peritidal packstone and stromatolitic boundstone (Fig. 4) indicates the repetitive occurrence of events affecting sediments after deposition and quiet periods, when the processes producing soft-sediment deformation structures were not active. Evidence of liquefaction and fracturing in inner platform settings excludes the role of mass movements (i.e. gravitational sliding), a process instead compatible with slope and proximal basinal settings. The observed facies associations and distribution of soft-sediment deformation structures, characterized by alternance of liquified stratigraphic intervals with undeformed sediments can be explained only by recurring events. This permits to exclude an origin related to episodic phenomena, such as meteoric impacts. The processes originating these structures must be related to events able to deform, liquify and fracture stratigraphic intervals, from 0.5 to 4.0 m thick, characterized by various degrees of cementation and separated by undeformed inner platform sediments. Considering bathymetric conditions, horizontal depositional profile and types of sedimentary structures, the origin of these structures requires recurring events able to repetitively shake sediments and induce liquefaction. The observed situations could be confidently ascribed to a succession of seismic shocks: earthquakes are the best candidate for discontinuously and repetitively producing the observed structures in the inner platform domain. Identification of seismically-triggered soft-sediment deformation structures in the inner platform permits to suggest that at least part of the observed deformation structures in the slope and basinal facies could be confidently related to seismic shocks, able to trigger slope failures, liquefaction of sediments and opening of extensional fractures, rapidly filled by sediments.

Palaeoseismic considerations

Repetitive occurrence of associations of diverse types of soft-sediment deformation structures produced at different physical conditions of the sediment in the same stratigraphic level indicates multiple events able to trigger deformations at different moments after deposition. Deposition of the studied succession close to a syndepositional normal fault (both on hangingwall and footwall) further supports that the origin of these structures should be related to multiple earthquakes, affecting the same layer more times at different physical states. Seismic studies on present-day conditions indicates that the development of evident soft-sediment deformation structures is generally related to events of Mw 5.0 or higher, this magnitude being considered the lowest able to trigger sediment liquefaction (Youd, 1977; Allen, 1986; Scott & Price, 1988; Audemard & De Santis, 1991; Galli, 2000). Earthquakes of higher magnitude are required for producing soft-sediment deformation structures at a distance greater than 15 to 20 km from the epicentre (Galli, 2000, indicates that about 80% of liquefaction occurs within 30 km from the epicentre): a magnitude higher than six is suggested for liquefaction at greater distances (e.g. Moretti *et al.*, 1995; Moretti & Tropeano, 1996; Blanc *et al.*, 1998). The presence of one of the numerous Norian faults close to the observed soft-sediment deformation structures indicates that their origin is compatible with earthquakes of magnitude Mw not lower than five. Multiple seismic events may also explain the high abundance of structures in defined stratigraphic intervals, as well as the presence of various types and generations of soft-sediment deformation structures affecting the same stratigraphic interval. Available data do not permit to constrain the possible distribution in depth of hypocentres: considering the position and normal kinematics of the Norian syndepositional fault, and occurrence of soft-sediment deformation mostly limited to the fault-controlled margin of the platform, a prevailing shallow hypocentral depth can be suggested. Actually, these conditions are expected to generate earthquakes responsible for less severe shaking, as well as liquefaction limited to the surroundings of the fault, with respect to deeper earthquakes that generally create more severe shaking across wider areas (Obermeier, 1996).

Some qualitative palaeo-seismic considerations are also possible, according to the reconstructed tectonic setting of the study area, in comparison with other extensional domains. In present-day extensional basins, such as Basin and Range (Bennett *et al.*, 2003), Crete (Nicol *et al.*, 2020) and Gulf of Corinth (Robertson *et al.*, 2020), extensional rate ranges roughly between less than 0.1 mm/year to about 5.0 mm/year (e.g. Robertson *et al.*, 2020), so that a wide range of net vertical tectonic displacement along faults can be expected. It is therefore possible to suggest only approximatively the expected rate and duration of tectonic activity along the Pizzo Formico syndepositional normal fault, as well as its throw. Studies of sets of normal faults indicate that maximum displacement–length ratio (D_{max}/L) in these faults has a variable range (Lathrop *et al.*, 2022), primarily between 10^{-1} and 10^{-2}, regardless of rock type (Schultz & Fossen, 2002). Robertson *et al.* (2020) recently calculated a D_{max}/L ratio from 0.03 to 0.27: because the Norian extensional fault in the Pizzo Formico area can be followed for about 3 km, it is possible to expect a throw roughly between 90 m and 810 m, values that are compatible with the observed geological setting. Of course, the throw of the observed normal fault in the study area (evaluated as about 150–200 m) results from many single seismic events, most of them generating earthquakes of a magnitude of five or higher, required to produce the observed soft-sediment deformation structures. According to Ferrill *et al.* (2008), D_{max}/L for total fault displacement, in general, is approximately 100 times D_{max}/L for single-event ruptures: according to these authors, single events have in general a D_{max}/L ratio ranging from 10^{-4} to 10^{-5} (with 8×10^{-5} average) for faults of a length ranging from 100 to 1000 m; for faults of a length from 1 to 100 km, D_{max}/L ratio results to be on average 7×10^{-5} of the fault length (Wells & Coppersmith, 1994). Considering a fault about 3000 m long, the average displacement of the Pizzo Formico normal fault (considering results of Ferrill *et al.*, 2008) is expected to be around 25 cm for each seismic event, on average. The resulting scenario is compatible with that observed for the normal fault developed south of Pizzo Formico, in terms of total fault displacement and numbers of events required. Distribution in time of seismic events (i.e. period of fault activity) cannot be constrained for the studied stratigraphic interval, but preservation of soft-sediment deformation structures for a significant thickness suggests a persistent tectonic instability for a relatively long period, characterized by extensional tectonics documented by the Norian development of intraplatform basins (Jadoul *et al.*, 1992).

CONCLUSIONS

Processes generating soft-sediment deformation structures are diverse, and the interpretation of these structures as genetically related to a specific type of event is not obvious. Therefore, identification of the triggering mechanisms of these structures must rely upon a detailed sedimentological study that considers not only the features of these structures, but also requires a definition of geological conditions existing at the time of deposition and deformation of sediments. The richer the information is, the more reliable may be the identification of genetic processes: it is therefore possible to exclude less plausible mechanisms according to sedimentological and local evidence, and select the most likely ones. This process may be more reliable when different coeval facies and depositional settings are affected by soft-sediment deformation structures, and their recurrence is abundant, so that interpretation could be more reliable: in those cases, it is necessary to identify a process that could be responsible for different structures in different environments, rather than thinking about diverse processes occurring contemporaneously in the same place, preferring (as usual, not only in geology) the simplest explanation with respect to more complex ones.

The observed soft-sediment deformation structures, associated with sedimentary dykes and brittle fractures, at the transition from inner platform to slope and proximal basin facies in the carbonate system of the Dolomia Principale, affected by syndepositional extensional tectonics, can be interpreted as produced by seismic shocks, which are able to explain the diverse structures here described. This identification of seismic shocks as the best candidate to explain the observed structures is not defined on the basis of a single type of soft-sediment deformation structure, but of the association of various structures and a complete sedimentological and stratigraphic study. Accordingly, most of the observed soft-sediment deformation structures (liquefaction and fluidization of cohesive carbonate sediments in diverse bathymetric conditions, from inner platform to the proximal slope, instability of slope facies, opening of fractures with the injection of plastically-deformed sediments, Neptunian dykes) can be confidently interpreted as related to seismic shocks (and, thus, interpretable as seismites), not only for their specific characteristics but mostly for their co-occurrence and for the regional setting in which they were formed. The set of diverse soft-sediment deformation structures observed in the study area, and interpreted as seismically-induced, thus may be considered as a reference for other geological settings where, in different subenvironments of a carbonate system affected by syndepositional tectonics, similar structures could be identified.

Links to three-dimensional digital outcrop geological models:

1 Example of soft-sediment deformation structures on the platform top (inner platform and margin facies; WGS84 coordinates 45.8465792 N, 9.9197040 E) https://poly.cam/capture/a068e97c-81e6-4fe3-8188-4f4ecc658a32

2 Example of soft-sediment deformation structures in basinal deposits (Zorzino Limestone) recorded in layers with a typical pseudonodular/boudinage aspect (WGS84 coordinates: 45.8403310 N, 9.9125022 E) https://poly.cam/capture/b37b9ffc-7fd3-4382-9966-a07d96c1a2fe

3 Aspects of the clinostratified slope breccias (south-western slope of Pizzo Formico, hanging-wall of the Norian syndepositional fault), with plastic clasts embedded in abundant lime-mudstone and packstone background; note dark plastic clasts exploded in small shreds within a light grey dolomitized lime-mudstone (WGS84 coordinates 45.8432113 N,9.9142849 E) https://poly.cam/capture/8898c3c6-f30e-4bbd-85d7-5e821dc337ea

4 Fractures in slope facies, embedded in plastic, dolomitized, lime-mudstone. Clasts are closely spaced with complementary margins, documenting an *in situ* brecciation, with partial displacement of the clasts, separated by soft-sediments (WGS84 coordinates 45.844716 N, 9.915646 E) https://poly.cam/capture/c5f1f82f-9658-4c98-af71-8389989ed803

ACKNOWLEDGEMENTS

This research integrates a long-lasting set of studies on the Dolomia Principale platform in the Lombardy Southern Alps of Italy, focusing on the role of syndepositional tectonics in its evolution. I am grateful to Flavio Jadoul for introducing me to the study of the fault-controlled carbonate platform of the Dolomia Principale and for sharing his long experience on this subject. The original manuscript benefitted from the constructive comments of three reviewers and of the Editor: their valuable comments are here warmly acknowledged.

DATA AVAILABILITY STATEMENT

The data that support the findings of this study are available from the corresponding author upon reasonable request.

REFERENCES

Allen, J.R.L. (1986) Earthquake magnitude-frequency, epicentral distance, and soft-sediment deformation in sedimentary basins. *Sediment. Geol.*, **46**, 67–75.

Alsop, G.I. and **Marco, S.** (2011) Soft-sediment deformation within seismogenic slumps of the Dead Sea Basin. *J. Struct. Geol.*, **33**, 433–457.

Alsop, G.I., **Marco, S.** and **Levi, T.** (2022) Recognising surface versus sub-surface deformation of soft-sediments: consequences and considerations for palaeoseismic studies. *J. Struct. Geol.*, **154**, 104493.

Assereto, R. and **Casati, P.** (1965) Revisione della stratigrafia permo-triassica della Val Camonica meridionale (Lombardia). *Rivista Italiana di Paleontologia e Stratigrafia*, **71**, 999–1097 (in Italian).

Audemard, F.A. and **De Santis, F.** (1991) Survey of liquefaction structures induced by recent moderate earthquakes. *Bull. Int. Assoc. Eng. Geol.*, **44**, 5–16.

Basilone, L. (2017) Seismogenic rotational slumps and translational glides in pelagic deep-water carbonates. Upper Tithonian-Berriasian of Southern Tethyan margin (W Sicily, Italy). *Sed. Geol.*, **356**, 1–14.

Basilone, L. (2022) Jurassic–Cretaceous intraplatform basins from NW Sicily fold and thrust belt: implications for oblique rifting of the Southern Tethyan margin. *Sed. Geol.*, **440**, 106255.

Bechstädt, T., **Brandner, R.**, **Mostler, H.** and **Schmidt, K.** (1978) Aborted rifting in the Triassic of the Eastern and Southern Alps. *Neues Jahrbuch für Geologie und Paläontologie Abhandlungen*, **156**, 157–178.

Bennett, R.A., **Wernicke, B.P.**, **Niemi, N.A.**, **Friedrich, A.M.** and **Davis, J.L.** (2003) Contemporary strain rates in the northern Basin and Range province from GPS data. *Tectonics*, **22**(2), 1008.

Berra, F. (1995) Stratigraphic evolution of a Norian intraplatform basin recorded in the Quattervals Nappe (Austroalpine, Northern Italy) and paleogeographic implications. *Eclogae Geol. Helv.*, **88**, 501–528.

Berra, F. and **Jadoul, F.** (1996) Norian serpulid and microbial bioconstructions: implication for the platform evolution in the Lombardy Basin (Southern Alps, Italy). *Facies*, **35**, 143–162.

Berra, F. and **Jadoul, F.** (1999) Stratigraphy, paleogeography and tectonic setting of the Norian succession of the Ortles Nappe (Central Austroalpine, Lombardy, Northern Italy). *Memorie di Scienze Geologiche dell'Università di Padova*, **51**, 78–89.

Berra, F., **Jadoul, F.** and **Anelli, A.** (2010) Environmental control on the end of the Dolomia Principale/Hauptdolomit depositional system in the Central Alps: coupling sea-level and climate changes. *Palaeogeogr. Palaeoclimatol. Palaeoecol.*, **290**, 138–150.

Bertotti, G. (1991) Early mesozoic extension and Alpine tectonics in the western Southern Alps: the geology of the area between Lugano and Menaggio (Lombardy, Northern Italy). *Mem. Sci. Geol. Padova*, **43**, 17–123.

Blanc, E.J.-P., **Blanc-Alétru, M.-C.** and **Mojon, P.-O.** (1998) Soft-sediment deformation structures interpreted as seismites in the uppermost Aptian to lowermost Albian transgressive deposits of the Chihuahua basin (Mexico). *Geol. Rundsh.*, **86**, 875–883.

Bonamini, E. and **Berra, F.** (2022) Resedimented limestones in fault-controlled basins (Zorzino Limestone, Southern Alps, Norian, Italy): facies types and depositional model. *Sed. Geol.*, **431**, 106106.

Bourrouilh, R., **Bourque, P.A.**, **Dansereau, P.**, **Bourrouilh-Le Jan, F.** and **Weyant, P.** (1998) Synsedimentary tectonics, mud-mounds and sea-level changes on a Palaeozoic carbonate platform margin: a Devonian Montagne Noire example (France). *Sed. Geol.*, **118**, 95–118.

Chen, J. and **Lee, H.S.** (2013) Soft-sediment deformation structures in Cambrian siliciclastic and carbonate storm deposits (Shandong Province, China): differential liquefaction and fluidization triggered by storm-wave loading. *Sed. Geol.*, **288**, 81–94.

Chough, S.K. and **Chen, J.** (2013) Generation of subsurface injection flow in a carbonate platform. *Geosci. J.*, **17**, 3–8.

Cirilli, S., **Iannace, A.**, **Jadoul, F.** and **Zamparelli, V.** (1999) Microbial-serpulid build-ups in the Norian-Rhaetian of the western Mediterranean area: ecological response of shelf margin communities to stressed environments. *Terra Nova*, **11**, 195–202.

Collinson, J. (1994) Sedimentary deformational structures. In: *The Geological Deformation of Sediments*, pp. 95–125. Springer Netherlands, Dordrecht.

Cozzi, A. (2002) Facies patterns of a tectonically-controlled Upper Triassic platform-slope carbonate depositional system (Carnian Prealps, Northeastern Italy). *Facies*, **47**, 151–178.

Cui, M., **Peng, N.**, **Liu, Y.**, **Wang, Z.**, **Li, C.**, **Xu, K.** and **Kuang, H.** (2022) Recognizing deformation origins: a review of deformation structures and hypothesis on the perspective of sediment consolidation. *Int. Geol. Rev.*, **65**, 1500–1523.

El Taki, H. and **Pratt, B.R.** (2012) Syndepositional tectonic activity in an epicontinental basin revealed by deformation of subaqueous carbonate laminites and evaporites: seismites in Red River strata (Upper Ordovician) of southern Saskatchewan, Canada. *Bull. Can. Petrol. Geol.*, **60**, 37–58.

Elliott, C.G. and **Williams, P.F.** (1988) Sediment slump structures: a review of diagnostic criteria and application to an example from Newfoundland. *J. Struct. Geol.*, **10**, 171–182.

Ettensohn, F.R., **Zhang, C.**, **Gao, L.** and **Lierman, R.T.** (2011) Soft-sediment deformation in epicontinental carbonates as evidence of paleoseismicity with evidence for a possible new seismogenic indicator: accordion folds. *Sed. Geol.*, **235**, 222–233.

Ferrill, D.A., **Smart, K.J.** and **Necsoiu, M.** (2008) Displacement-length scaling for single-event fault ruptures: insights from Newberry Springs Fault Zone and implications for fault zone structure. *Geol. Soc. Lond. Spec. Publ.*, **299**, 113–122.

Fruth, I. and **Scherreiks, R.** (1984) Hauptdolomit—sedimentary and paleogeographic models (Norian, Northern Calcareous Alps). *Geologische Rundschau*, **73**, 305–319.

Galli, P. (2000) New empirical relationships between magnitude and distance for liquefaction. *Tectonophysics*, **324**, 169–187.

Grammer, G.M., **Crescini, C.M.**, **McNeill, D.F.** and **Taylor, L.H.** (1999) Quantifying rates of syndepositional marine cementation in deeper platform environments-new insight into a fundamental process. *J. Sediment. Res.*, **69**, 202–207.

Heezen, B.C. and **Ewing, W.M.** (1952) Turbidity currents and submarine slumps, and the 1929 Grand Banks [Newfoundland] earthquake. *Am. J. Sci.*, **250**, 849–873.

Hou, Z., **Chen, S.**, **Zhang, S.** and **Yang, H.** (2020) Sedimentary deformation features as evidence for paleoseismic events in the middle Eocene in the Dongying Depression of the southern Bohai Bay Basin, eastern China. *Can. J. Earth Sci.*, **57**, 954–970.

Hurst, A., **Cartwright, J.** and **Duranti, D.** (2003) Fluidization structures produced by upward injection of sand through a sealing lithology. *Geol. Soc. Lond. Spec. Publ.*, **216**, 123–138.

ISPRA. (2012) Carta geologica d'Italia 1:50.000 - Foglio 077 CLUSONE.

Jadoul, F. (1985) Stratigrafia e paleogeografia del Norico nelle Prealpi Bergamasche occidentali. *Rivista Italiana di Paleontologia e Stratigrafia*, **91**, 479–512.

Jadoul, F., **Berra, F.** and **Frisia, S.** (1992) Stratigraphic and paleogeographic evolution of a carbonate platform in an extensional tectonic regime: the example of the Dolomia Principale in Lombardy (Italy). *Rivista Italiana di Paleontologia e Stratigrafia*, **98**, 29–43.

Jones, M. (1994) Mechanical principles of sediment deformation. In: *The Geological Deformation of Sediments*, pp. 37–71. Springer Netherlands, Dordrecht.

Kirkland, D.W. and **Anderson, R.Y.** (1970) Microfolding in the Castile and Todilto evaporites, Texas and New Mexico. *Geol. Soc. Am. Bull.*, **81**, 3259–3282.

Kondo, H. and **Owen, L.A.** (2013) Paleoseismology. In: *Treatise on Geomorphology* (Ed Shroder, J.F.), pp. 267–299. Academic Press, Cambridge.

Lathrop, B., **Jackson, C.**, **Bell, R.E.** and **Rotevatn, A.** (2022) Displacement/Length scaling relationships for normal faults; a review, critique, and revised compilation. *Front. Earth Sci.*, **10**, 907543.

Maltman, A. (1994) Deformation structures preserved in rocks. In: *The Geological Deformation of Sediments*, pp. 261–307. Springer Netherlands, Dordrecht.

Marcoux, J., **Baud, A.**, **Ricou, L.E.**, **Gaetani, M.**, **Krystyn, L.**, **Bellion, Y.**, **Guiraud, R.**, **Besse, J.**, **Gallet, Y.**, **Jaillard, E.**

and **Moreau, C.** (1993) Late Norian (215-212 Ma). Atlas Tethys Palaeoenvironmental Maps. Explanatory Notes. pp. 35–54.

Moretti, M. and **Tropeano, M.** (1996) Strutture sedimentarie deformative (sismiti) nei depositi Tirreniani di Bari. *Mem. Soc. Geol. It.*, **51**, 485–500.

Moretti, M., **Pieri, P.**, **Tropeano, M.** and **Walsh, N.** (1995) Tyrrhenian seismites in Bari Area (Murge-Apulian foreland). Atti Convegno 'Terremoti in Italia' - Previsione e prevenzione dei danni-Accademia Nazionale dei Lincei, 211–216.

Moretti, M., **Pieri, P.** and **Tropeano, M.** (2002) Late Pleistocene soft-sediment deformation structures interpreted as seismites in paralic deposits in the City of Bari (Apulian foreland, southern Italy). *Geol. Soc. Am. Spec. Pap.*, **359**, 75–85.

Moretti, M., **van Loon, A.T.**, **Liu, M.** and **Wang, Y.** (2014) Restrictions to the application of 'diagnostic' criteria for recognizing ancient seismites. *J. Palaeogeogr.*, **3**, 162–173.

Morsilli, M., **Giona Bucci, M.**, **Gliozzi, E.**, **Lisco, S.** and **Moretti, M.** (2020) Sedimentary features influencing the occurrence and spatial variability of seismites (late Messinian, Gargano Promontory, southern Italy). *Sed. Geol.*, **401**, 105628.

Nicol, A., **Mouslopoulou, V.**, **Begg, J.** and **Oncken, O.** (2020) Displacement accumulation and sampling of paleoearthquakes on active normal faults of Crete in the eastern Mediterranean. *Geochem. Geophys. Geosyst.*, **21**, e2020GC009265.

Obermeier, S.F. (1996) Use of liquefaction-induced features for paleoseismic analysis. An overview of how seismic liquefaction features can be distinguished from other features and how their regional distribution and properties of source sediment can be used to infer the location and strength of Holocene paleo-earthquakes. *Eng. Geol.*, **44**, 1–76.

Obermeier, S.F. (2009) Using liquefaction-induced and other soft-sediment features for paleoseismic analysis. *Int. Geophys.*, **95**, 497–564.

Owen, G. and **Moretti, M.** (2011) Identifying triggers for liquefaction-induced soft-sediment deformation in sands. *Sed. Geol.*, **235**, 141–147.

Pando, M.A., **Sandoval, E.A.** and **Catano, J.** (2012) Liquefaction susceptibility and dynamic properties of calcareous sands from Cabo Rojo, Puerto Rico. In: *Proceedings of the 15th World Conference on Earthquake Engineering*, the conference was held in Lisboa, Portugal, proceedings printed by Curran Associates, Inc., NY, U.S.A., 2012, 30501–30510.

Picotti, P. and **Pini, G.** (1988) Tettonica sinsedimentaria norica nel settore compreso tra il Lago d'Idro e il Lago di Garda. *Rendiconti della Società Geologica Italiana*, **11**, 225–230 (in Italian).

Pratt, B.R. (1994) Seismites in Mesoproterozoic Altyn formation (Belt Supergroup), Montana: a test for tectonic control of peritidal carbonate cyclicity. *Geology*, **22**, 1091–1094.

Robertson, J., **Roberts, G.P.**, **Iezzi, F.**, **Meschis, M.**, **Gheorghiu, D.M.**, **Sahy, D.**, **Bristow, C.** and **Sgambato, C.** (2020) Distributed normal faulting in the tip zone of the South Alkyonides Fault System, Gulf of Corinth, constrained using 36Cl exposure dating of late-Quaternary wave-cut platforms. *J. Struct. Geol.*, **136**, 104063.

Sandoval, E.A. and **Pando, M.A.** (2012) Experimental assessment of the liquefaction resistance of calcareous biogenous sands. *Earth Sci. Res. J.*, **16**, 55–63.

Schultz, R.A. and **Fossen, H.** (2002) Displacement–length scaling in three dimensions: the importance of aspect ratio and application to deformation bands. *J. Struct. Geol.*, **24**, 1389–1411.

Scott, B. and **Price, S.** (1988) Earthquake-induced structures in young sediments. *Tectonophysics*, **147**, 165–170.

Seed, H.B. and **Idriss, I.M.** (1967) Analysis of soil liquefaction: Niigata earthquake. *J. Soil Mech. Found. Div.*, **93**, 83–108.

Seilacher, A. (1969) Fault-graded beds interpreted as seismites. *Sedimentology*, **13**, 155–159.

Shanmugam, G. (2016) The seismite problem. *J. Palaeogeogr.*, **5**, 318–362.

Shanmugam, G. (2017) Global case studies of soft-sediment deformation structures (SSDS): definitions, classifications, advances, origins, and problems. *J. Palaeogeogr.*, **6**, 251–320.

Spalluto, L., **Moretti, M.**, **Festa, V.** and **Tropeano, M.** (2007) Seismically-induced slumps in Lower-Maastrichtian peritidal carbonates of the Apulian Platform (southern Italy). *Sed. Geol.*, **196**, 81–98.

Trombetta, G.L. (1992) Tettonica trastensiva, bacini di pull-apart e sedimentazione nel Norico delle Prealpi Bresciane. *Atti Ticinensi di Scienze della Terra*, **35**, 127–137 (in Italian).

Trombetta, G.L. and **Claps, M.** (1995) Sedimentology and depositional evolution of a platform-basin system: the example of the Ledro Valley intra-platform basin (Norian-Rhaetian, Southern Alps). *Mem. Sci. Geol.*, **47**, 31–44.

Van Loon, A.J. (2009) Soft-sediment deformation structures in siliciclastic sediments: an overview. *Geologos*, **15**, 3–55.

Wallace, K. and **Eyles, N.** (2015) Seismites within Ordovician–Silurian carbonates and clastics of Southern Ontario, Canada and implications for intraplate seismicity. *Sed. Geol.*, **316**, 80–95.

Wells, D.L. and **Coppersmith, K.J.** (1994) New empirical relationships among magnitude, rupture length, rupture width, rupture area, and surface displacement. *Bull. Seismol. Soc. Am.*, **84**, 974–1002.

Wendt, J. (2017) A unique fossil record from neptunian sills: the world's most extreme example of stratigraphic condensation (Jurassic, western Sicily). *Acta Geol. Polonica*, **67**, 163–199.

Youd, T.L. (1977) Discussion of 'Brief review of liquefaction during earthquakes in Japan' by E. Kuribayashi and T. Taatsuoka. *Soils Found.*, **17**, 82–85.

Zamparelli, V., **Cirilli, S.**, **Iannace, A.**, **Jadoul, F.**, **Colacicchi, R.** and **Parisi, G.** (1999) Palaeotectonic and palaeoceanographic controls on microbial–serpulid communities in the Norian–Rhaetian carbonates of Italy: a synthesis. Bioevents and Integrated Stratigraphy of the Triassic and the Jurassic in Italy. *Paleopelagos Spec. Publ.*, **3**, 7–84.

Zhang, K., **Wang, Y.**, **Zhang, G.**, **Xu, T.**, **Xiong, W.**, **Wang, S.**, **Ma, J.** and **Sun, T.** (2022) Discovery of Seismites in the Carboniferous Formation of the Shibei Sag (China) and Its Petroleum Geological Significance. *Minerals*, **12**, 1560.

Manuscript received 8 February 2023; revision accepted 25 October 2023